Structural Analysis of UDP-Sugar Binding to UDP-Galactose 4-Epimerase from *Escherichia coli*[†,‡]

James B. Thoden, Adrian D. Hegeman, Gary Wesenberg, Marie C. Chapeau, Perry A. Frey, and Hazel M. Holden*

Institute for Enzyme Research, The Graduate School, and Department of Biochemistry, College of Agricultural and Life Sciences, University of Wisconsin−Madison, 1710 University Avenue, Madison, Wisconsin 53705

Received January 3, 1997; Revised Manuscript Received March 20, 1997[⊗]

ABSTRACT: UDP-galactose 4-epimerase from *Escherichia coli* catalyzes the interconversion of UDP-galactose and UDP-glucose through the transient reduction of the tightly bound cofactor NAD^+. The enzyme is unique among the NAD^+-dependent enzymes in that it promotes stereospecific reduction of the cofactor but nonstereospecific hydride return during normal catalysis. In addition to hydride transfer, the reaction mechanism of epimerase involves two key features: the abstraction of a proton from the 4′-hydroxyl group of glucose or galactose by an active site base and the rotation of a 4-ketopyranose intermediate in the active site pocket. To address the second issue of movement within the active site, the X-ray structures of reduced epimerase complexed with UDP-mannose, UDP-4-deoxy-4-fluoro-α-D-galactose, or UDP-4-deoxy-4-fluoro-α-D-glucose have been determined and refined to 1.65, 1.8, and 1.65 Å resolution, respectively. A comparison of these models to that of the previously determined epimerase/NADH/UDP-glucose abortive complex reveals that the active site accommodates the various sugars by simple rearrangements of water molecules rather than by large changes in side chain conformations. In fact, the polypeptide chains for all of the epimerase/NADH/UDP-sugar complexes studied thus far are remarkably similar and can be superimposed with root-mean-square deviations of not greater than 0.24 Å. The only significant differences between the various enzyme/UDP-sugar models occur in two of the dihedral angles defining the conformation of the UDP-sugar ligands.

UDP-galactose 4-epimerase, hereafter referred to as epimerase, plays a critical role in galactose metabolism by catalyzing the interconversion of UDP-galactose[1] and UDP-glucose. As isolated from *Escherichia coli*, the epimerase is a homodimer with each subunit containing 338 amino acid residues and one tightly bound NAD^+ or NADH moiety (Wilson & Hogness, 1969; Lemaire & Müller-Hill, 1986, Thoden *et al.*, 1996c). X-ray crystallographic investigations of the bacterial enzyme have shown that each subunit folds into two distinct structural units, the N-terminal nucleotide binding motif and the smaller C-terminal domain (Bauer *et al.*, 1992; Thoden *et al.*, 1996c). The N-terminal region consists of seven strands of parallel β-pleated sheet flanked on either side by a total of six α-helices arranged in a modified "Rossmann-type" fold. The C-terminal domain is simpler with five β-strands and four α-helical regions. As shown in Figure 1, the active site is located at the domain−domain interface (Thoden *et al.*, 1996a−c). Within recent years, it has become apparent that the epimerase belongs to the superfamily of "short-chain" dehydrogenases which contain a characteristic Tyr-Lys couple thought to function in catalysis (Baker & Blasco, 1992; Holm *et al.*, 1994; Thoden *et al.*, 1996c). Other enzymes in this family, for which three-dimensional structures are available, include 3α,-20β-hydroxysteroid dehydrogenase (Ghosh *et al.*, 1991, 1994a,b), dihydropteridine reductase (Varughese *et al.*, 1992, 1994), 7α-hydroxysteroid dehydrogenase (Tanaka *et al.*, 1996a), mouse lung carbonyl reductase (Tanaka *et al.*, 1996b), and 17β-hydroxysteroid dehydrogenase (Ghosh *et al.*, 1995; Azzi *et al.*, 1996). The epimerase is somewhat unique among the other members of the above-mentioned short-chain dehydrogenases, however, in that the dinucleotide is tightly bound such that its removal results in irreversible denaturation of the enzyme (Frey, unpublished results; Thoden *et al.*, 1996a).

Since the initial report of epimerase activity by Caputto *et al.* (1949), a substantial research effort has been directed toward understanding its fascinating catalytic mechanism. All presently available biochemical and kinetic data suggest that the reaction mechanism, as outlined in Scheme 1, proceeds through the abstraction of the C4 hydroxyl hydrogen of the sugar by an active site base and the transfer of a hydride from C4 to the *B*-side of NAD^+, resulting in a 4-ketopyranose intermediate and a reduced cofactor. The 4-ketopyranose intermediate is thought to rotate in the active site in a manner that allows the return of the hydride from NADH to the opposite face of the sugar (Kang *et al.*, 1975). This nonstereospecificity displayed by epimerase is in sharp contrast to the NAD^+-dependent dehydrogenases that undergo stereospecific hydride transfer (Walsh, 1979).

[†] This research was supported in part by grants from the NIH (DK47814 to H.M.H. and GM30480 to P.A.F.) and the NSF (BIR-9317398 shared instrumentation grant to Ivan Rayment).

[‡] X-ray coordinates have been deposited in the Brookhaven Protein Data Bank (1UDA, 1UDB, and 1UDC).

* To whom correspondence should be addressed.

[⊗] Abstract published in *Advance ACS Abstracts,* May 15, 1997.

[1] Abbreviations: CHES, 2-(cyclohexylamino)ethanesulfonic acid; UDP-glucose, uridine 5′-diphosphate glucose; UDP-galactose, uridine 5′-diphosphate galactose; UDP-mannose, uridine 5′-diphosphate mannose; UDP-fglu, uridine 5′-diphosphate 4-deoxy-4-fluoro-α-D-glucose; UDP-fgal, uridine 5′-diphosphate 4-deoxy-4-fluoro-α-D-galactose; UDP, uridine 5′-diphosphate; UMP, uridine 5′-monophosphate; TMP, thymidine 5′-monophosphate; UDP-TEMPO, uridine 5′-diphosphate 4-hydroxy-2,2,6,6-tetramethylpiperidine-1-oxyl.

S0006-2960(97)00025-1 CCC: $14.00

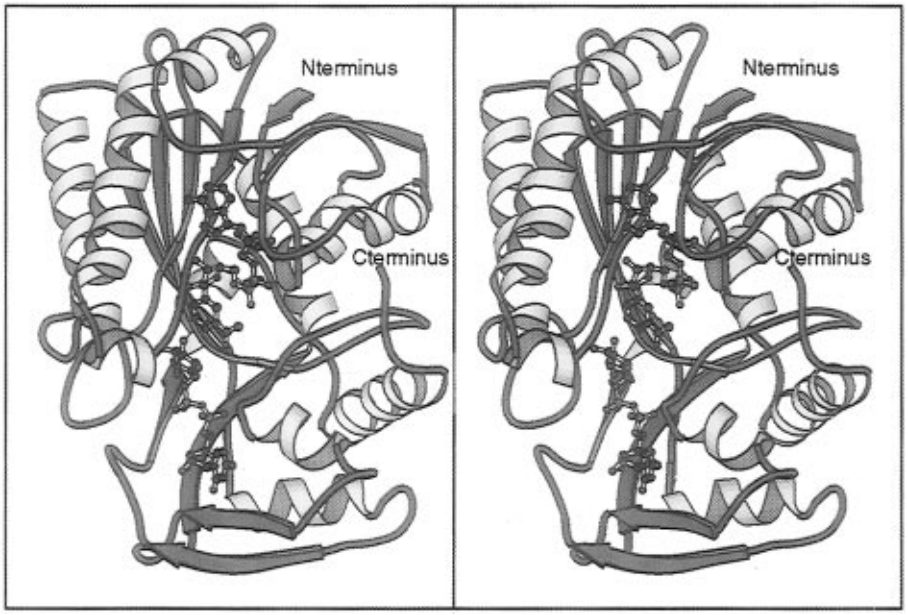

FIGURE 1: Ribbon representation of the epimerase subunit. X-ray coordinates employed for this figure were based on the structural determination of the epimerase/NADH/UDP-glucose abortive complex (Thoden *et al.*, 1996b). The NADH and UDP-glucose molecules are displayed in ball-and-stick representations. This figure and Figures 2, 4, 6, 8, and 10 were prepared with the software package MOLSCRIPT (Kraulis, 1991).

Scheme 1: Proposed Reaction Mechanism for UDP-Galactose 4-Epimerase

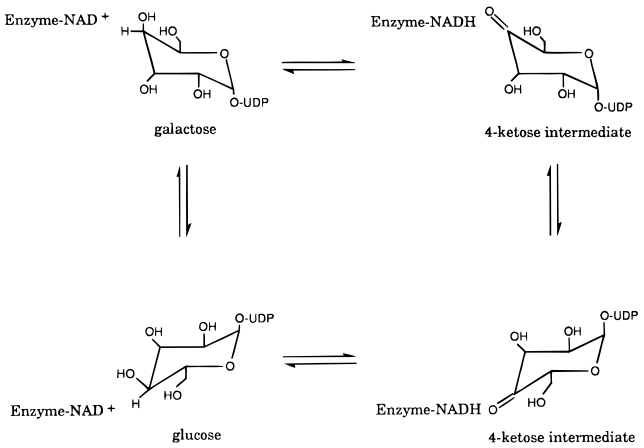

There are two important questions concerning the epimerase reaction mechanism that have been the focus of recent structural and biochemical studies: the location and identity of the catalytic base and the ability of the sugar substrate to rotate in the active site cleft. In an effort to identify the active site base, the three-dimensional structure of the epimerase/NADH/UDP-glucose abortive complex was recently determined to a nominal resolution of 1.8 Å (Thoden *et al.*, 1996b). As can be seen from Figure 2, the glucose and the dinucleotide are positioned correctly within the binding cleft for *B*-side specific hydride transfer. However, there are no "classical" enzymatic bases such as aspartates, glutamates, or histidines near the hexose; rather O^{γ} of Ser 124 is positioned at 2.6 Å from the 4′-hydroxyl group of the sugar. Reaction mechanisms involving both Ser 124 and Tyr 149 have now been proposed, and site-directed mutagenesis experiments designed to test the various hypotheses are presently underway (Thoden *et al.*, 1996c, unpublished results).

While these molecular biological studies are shedding light on the identity of the active site base, the ability of the epimerase active site to accommodate various sugars and to allow free rotation of the 4-ketopyranose intermediate is less well understood. Obviously one of the critical candidates for additional structural studies is the epimerase/NADH/UDP-galactose abortive complex. All experiments designed to produce such a crystalline complex, however, have been unsuccessful thus far (Thoden *et al.*, 1996b). These attempts have included reduction of the enzyme with dimethylamine/borane complex in the presence of UDP-galactose, UDP, UMP, or TMP and exchange of these nucleotides with UDP-galactose. In each case, the resulting electron density maps have clearly indicated the presence of UDP-glucose, rather than UDP-galactose, in the epimerase active site (Thoden *et al.*, 1996b).

In a parallel effort to more fully explore the binding of UDP-sugars to epimerase, the substrate analogs UDP-4-deoxy-4-fluoro-α-D-galactose and UDP-4-deoxy-4-fluoro-α-D-glucose were recently synthesized by Chapeau and Frey (1994). Here we report the three-dimensional structures of epimerase complexed with these compounds. Additionally, the high-resolution structure of epimerase with bound UDP-mannose has been determined and is also described here. While UDP-mannose is not a substrate for the enzyme, it does reduce the dinucleotide cofactor (Nelsestuen & Kirkwood, 1971). Taken together, these X-ray structural investigations more fully address the issue of substrate mobility in the active site. Furthermore, while the fluorinated carbohydrates did not bind in the expected orientation within the epimerase active site, their study has provided insight into the necessity of proper hydrogen bonding between the natural substrates and the protein.

MATERIALS AND METHODS

Materials. The UDP-mannose employed in the crystallization trials was purchased from Sigma. The UDP-fgal and UDP-fglu compounds, synthesized according to the method of Chapeau and Frey (1994), were further purified for crystallization trials by HPLC.

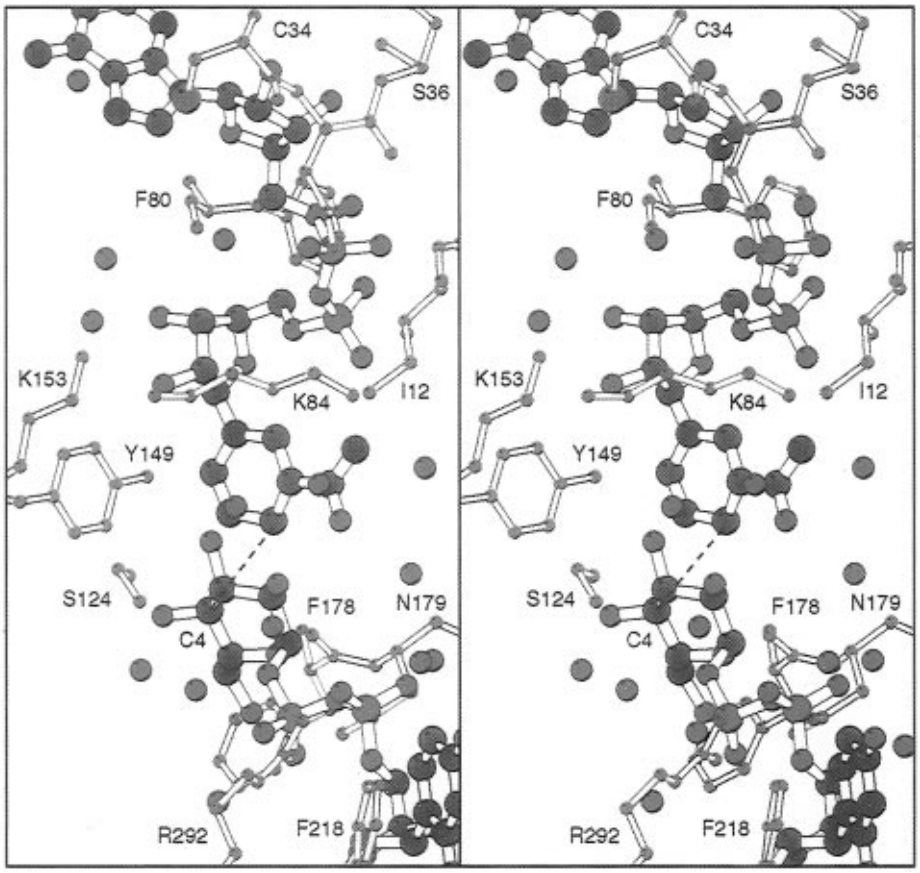

FIGURE 2: Close-up view of the active site for the epimerase/NADH/UDP-glucose abortive complex. Atoms corresponding to the nucleotides and the protein are displayed in standard colors and black, respectively. The positions of ordered water molecules are indicated by the red spheres. Note the close approach of O^{γ} of Ser 124 to the 4′-hydroxyl group of the UDP-glucose substrate. The black dashed line indicates the direction of hydride transfer from C4 of the sugar to C4 of the dinucleotide.

Purification and Crystallization Procedures. Recombinant UDP-galactose 4-epimerase was expressed in *E. coli* and purified according to previously published procedures (Thoden *et al.*, 1996a). Although crystals of the oxidized enzyme with bound UDP-sugars could be grown, they were always severely twinned. It was noted, however, that reduction of the dinucleotide NAD^+ to NADH resulted in the production of large single crystals. Consequently, for each protein/UDP-sugar complex, the epimerase was first reduced before crystallization trials. Conditions varied slightly with each UDP-sugar employed. For the protein/UDP-mannose complex, the epimerase, in 10 mM potassium phosphate (pH 7.0), was first incubated with the reducing agent, 50 mM dimethylamine/borane complex, for 2 h at room temperature. Subsequently, UDP-mannose was added to a concentration of 10 mM. The reaction was allowed to continue for 2 h after which time additional reducing agent was added to a concentration of 150 mM. The reaction was incubated overnight at 4 °C and then dialyzed against 10 mM potassium phosphate (pH 8.0) for 24 h at 4 °C. For the protein/UDP-fglu and UDP-fgal complexes, the respective UDP-fluorosugars, at 2 mM, were first incubated with separate samples of the epimerase in 10 mM potassium phosphate (pH 8.0) for 45 min at room temperature. Dimethylamine/borane complex was then added to each sample in three additions over 2 h to a concentration of 200 mM. These reactions were incubated overnight at 4 °C and next subjected to multiple rounds of dilution with buffer (10 mM potassium phosphate, pH 8.0) and concentration by ultrafiltration (Centricon 20) until a net 60-fold dilution of nonprotein components had been achieved. All samples were concentrated to 35−45 mg/mL for crystallization trials; additional UDP-mannose was added to a final concentration of 10 mM while additional UDP-fluorosugars were added to final concentrations of 2 mM.

Large single crystals of all three enzyme/UDP-sugar complexes were grown by the hanging drop method of vapor diffusion against 20−25% poly(ethylene glycol) 8000, 250−500 mM NaCl, and 50 mM CHES (pH 9.0) at 4 °C. Crystals typically appeared within 6−12 h, and growth was generally complete within 4−5 days. The crystals all belonged to the trigonal space group $P3_221$ with unit cell dimensions of $a = b = 83.5$ Å and $c = 108.9$ Å and one subunit per asymmetric unit. These crystals were isomorphous to those previously described for the NADH/UDP-glucose abortive complex (Thoden *et al.*, 1996b).

X-ray Data Collection and Processing. Prior to X-ray data collection, the crystals were transferred to 25% poly(ethylene glycol) 8000, 750 mM NaCl, 50 mM CHES (pH 9.0), 10 mM UDP-sugar, and 20% ethylene glycol. Each crystal was suspended in a thin film of this cryoprotectant solution in a loop of fine surgical thread and flash-cooled in a nitrogen stream. All X-ray data were collected at −150 °C with a Siemens HI-STAR area detector system equipped with long Supper double-focusing mirrors. The X-ray source was Cu Kα radiation from a Rigaku RU200 rotating anode generator operated at 50 kV and 90 mA and equipped with a 300 μm focal cup. Only one crystal was required per X-ray data set. The X-ray data were processed with the data reduction software package SAINT (Siemens Analytical X-ray Instru-

Table 1: Intensity Statistics for the Overall Data Sets and for the Higher Resolution Ranges (Å)

	UDP-mannose		UDP-4-deoxy-4-fluorogalactose		UDP-4-deoxy-4-fluoroglucose	
	overall	1.73−1.65	overall	1.88−1.80	overall	1.73−1.65
no. of measurements	160336	11518	120477	9159	124280	8489
no. of independent reflections	50521	5849	39033	4283	49619	5317
completeness of data (%)	95	89	92	83	93	81
average intensity	3190	357	3579	693	2428	117
average σ	163	130	267	319	95	41
R-factor[a] (%)	3.3	18.2	4.3	21.6	5.1	23.0

[a] $R\text{-factor} = (\sum|I - \bar{I}|/\sum I) \times 100$.

Table 2: Least-Squares Refinement Statistics for the Epimerase/Sugar Complexes

	mannose	fluorogalactose	fluoroglucose
resolution limits (Å)	30.0−1.65	30.0−1.80	30.0−1.65
R-factor (%)[a]	17.7	18.8	17.9
no. of reflections used	50521	39033	49616
no. of protein atoms	2706	2706	2706
no. of solvent atoms	584	575	589
weighted rmsd from ideality			
bond length (Å)	0.013	0.015	0.010
bond angle (deg)	2.29	2.67	2.15
planarity (trigonal) (Å)	0.009	0.009	0.006
planarity (other planes) (Å)	0.013	0.015	0.012
torsional angle (deg)[b]	14.7	14.9	14.7
average *B*-factors (Å^2)			
backbone atoms	15.0	16.8	23.0
all atoms	20.8	23.3	29.3

[a] $R\text{-factor} = \sum|F_o - F_c|/\sum|F_o|$, where F_o is the observed structure factor amplitude and F_c is the calculated structure factor amplitude. [b] The torsional angles were not restrained during the refinement.

ments), or XDS (Kabsch, 1988a,b), and scaled with the program XCALIBRE (G. Wesenberg and I. Rayment, unpublished results). Relevant X-ray data collection statistics for the three crystalline complexes can be found in Table 1.

Structural Determination. The previously solved structure of the epimerase/NADH/UDP-glucose complex (Thoden *et al.*, 1996b) served as the starting model for least-squares refinements of the three epimerase/UDP-sugar complexes described here. The software package TNT (Tronrud *et al.*, 1987) was employed for the refinements with ideal stereochemistries of the NADH, UDP, and sugar moieties based on the small molecule structural determinations of Reddy *et al.* (1981), Viswamitra *et al.* (1979), Glasfeld *et al.* (1988), and Lonchambon *et al.* (1976). Alternate cycles of manual model building with the program FRODO (Jones, 1985) and least-squares refinement reduced the *R*-factors to 17.7% (1.65 Å resolution), 18.8% (1.8 Å resolution), and 17.9% (1.65 Å resolution) for the epimerase/NADH/UDP-mannose, epimerase/NADH/UDP-fgal, and epimerase/NADH-fglu complexes, respectively. Ramachandran plots demonstrate that all non-glycinyl main chain dihedral angles lie within or near the allowed regions with the exception of Phe 178. In each complex, this residue adopts average ϕ,ψ angles of 95.8° and 113.1°, respectively. Previous studies have shown that the side chain conformation of Phe 178, like that of Phe 218, is dependent upon the oxidation state of the dinucleotide (Thoden *et al.*, 1996a).

Relevant refinement statistics are given in Table 2. The electron density maps for all three enzyme/NADH/UDP-sugar complexes were very well defined with only the following side chains showing some slight disorder: Lys 92, Glu 95, Glu 225, Lys 253, Lys 282, and Glu 293 (epimerase/NADH/UDP-mannose), Gln 22, Glu 95, Gln 146, Lys 165, Lys 278, and Glu 293 (epimerase/NADH/UDP-fgal), and Gln 22, Glu 95, Asp 130, Gln 146, Glu 225, Lys 278, and Lys 282 (epimerase/NADH/UDP-fglu). In addition, the electron density corresponding to residue 131 in the enzyme/NADH/UDP-mannose complex appeared more like a glutamine than an asparagine.

RESULTS

Description of the Epimerase/NADH/UDP-Mannose Complex. UDP-galactose 4-epimerase is specific for UDP-glucose and UDP-galactose substrates. Interestingly, while UDP-mannose is not a substrate for the enzyme, Nelsestuen and Kirkwood (1971) demonstrated that it reduces the dinucleotide. Note that mannose, a diastereomer of glucose, differs only in the configuration about C2 of the hexose.

A portion of the electron density map corresponding to the bound UDP-mannose is shown in Figure 3a. As can be seen, the electron density is unambiguous. Average *B*-values for the protein, the UDP-mannose and NADH molecules, and the solvent are 21.9, 13.1, and 38.4 Å^2, respectively. The polypeptide chains for the epimerase/NADH/UDP-mannose model and the epimerase/NADH/UDP-glucose abortive complex are strikingly similar such that the α-carbons for the two structures coincide with a root-mean-square deviation of 0.18 Å. The only regions where the two polypeptide chain backbones differ somewhat in these models are delineated by Ala 208 to Asp 232 and Pro 290 to Tyr 299 where the α-carbons correspond with a root-mean-square deviation of 0.48 Å. A superposition of these regions, along with the bound nucleotides, is displayed in Figure 4. Note that the positions of Ser 124, Tyr 149, and Lys 153 are identical, within coordinate error, between the two protein/UDP-sugar complexes.

If the UDP-mannose were to bind in an identical position to that observed for the natural glucose substrate, its 2′-hydroxyl group would be located at 2.0 Å from the amide nitrogen of the carboxamide group of NADH. To alleviate this close contact, both translational and rotational changes occur in the UDP-mannose molecule, relative to the UDP-glucose substrate. Specifically, the positions of the backbone α- and β-phosphorus atoms of the UDP-glucose and UDP-mannose ligands differ by 0.46 and 0.89 Å, respectively. In addition, the two dihedral angles defined by the α,β-bridging oxygen, the β-phosphorus, the glycosyl oxygen, and the hexose C1 and by the β-phosphorus, the glycosyl oxygen, the hexose C1, and C2 differ by approximately 39° and 49°, respectively. As a consequence of these translational and torsional changes, the C4 position of the mannose, relative to that observed for the glucose, is displaced by 1.7 Å within the active site cleft and the 4′-hydroxyl group is located at 5.5 Å rather than 2.6 Å from O^{γ} of Ser 124. Interestingly,

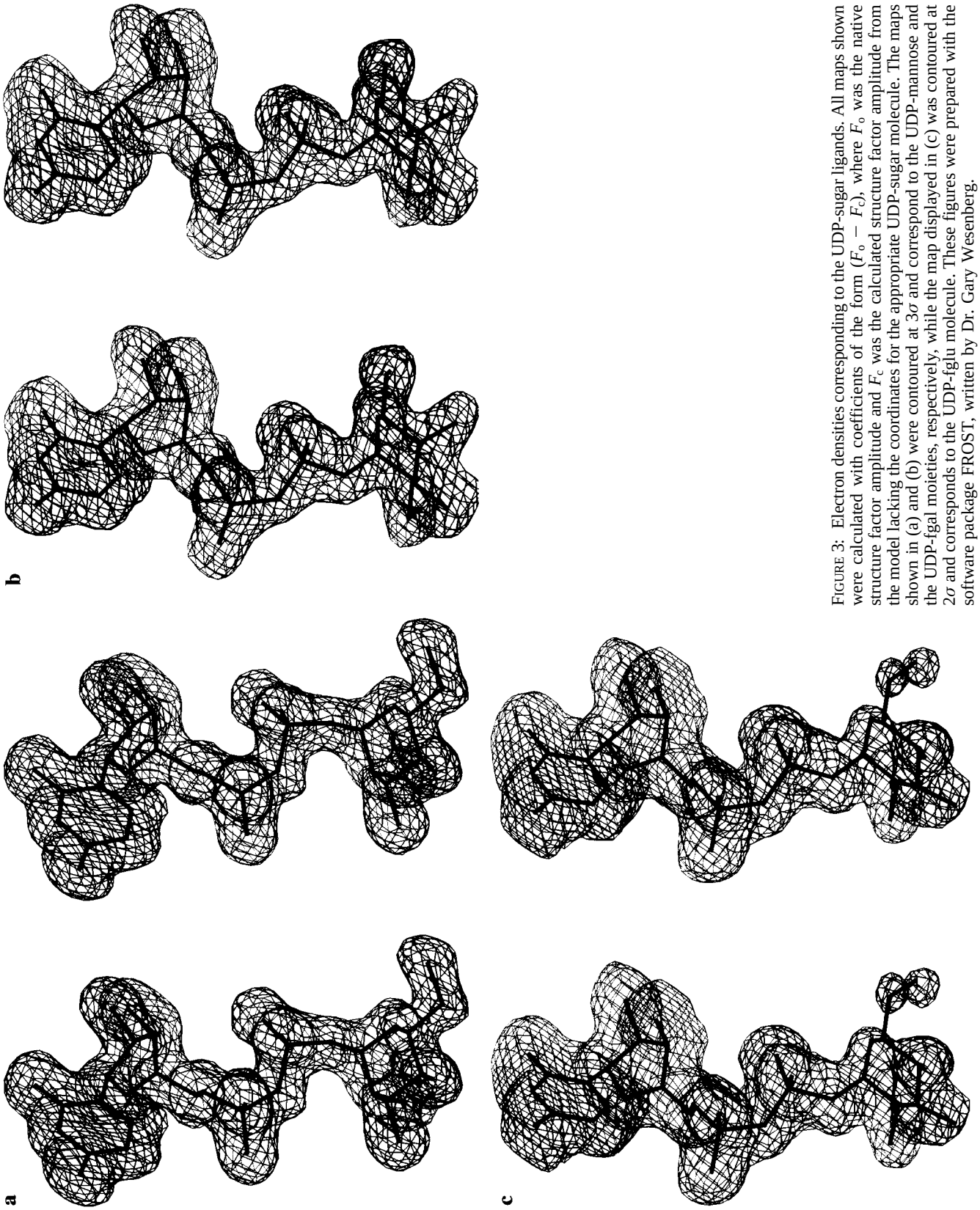

FIGURE 3: Electron densities corresponding to the UDP-sugar ligands. All maps shown were calculated with coefficients of the form $(F_o - F_c)$, where F_o was the native structure factor amplitude and F_c was the calculated structure factor amplitude from the model lacking the coordinates for the appropriate UDP-sugar molecule. The maps shown in (a) and (b) were contoured at 3σ and correspond to the UDP-mannose and the UDP-fgal moieties, respectively, while the map displayed in (c) was contoured at 2σ and corresponds to the UDP-fglu molecule. These figures were prepared with the software package FROST, written by Dr. Gary Wesenberg.

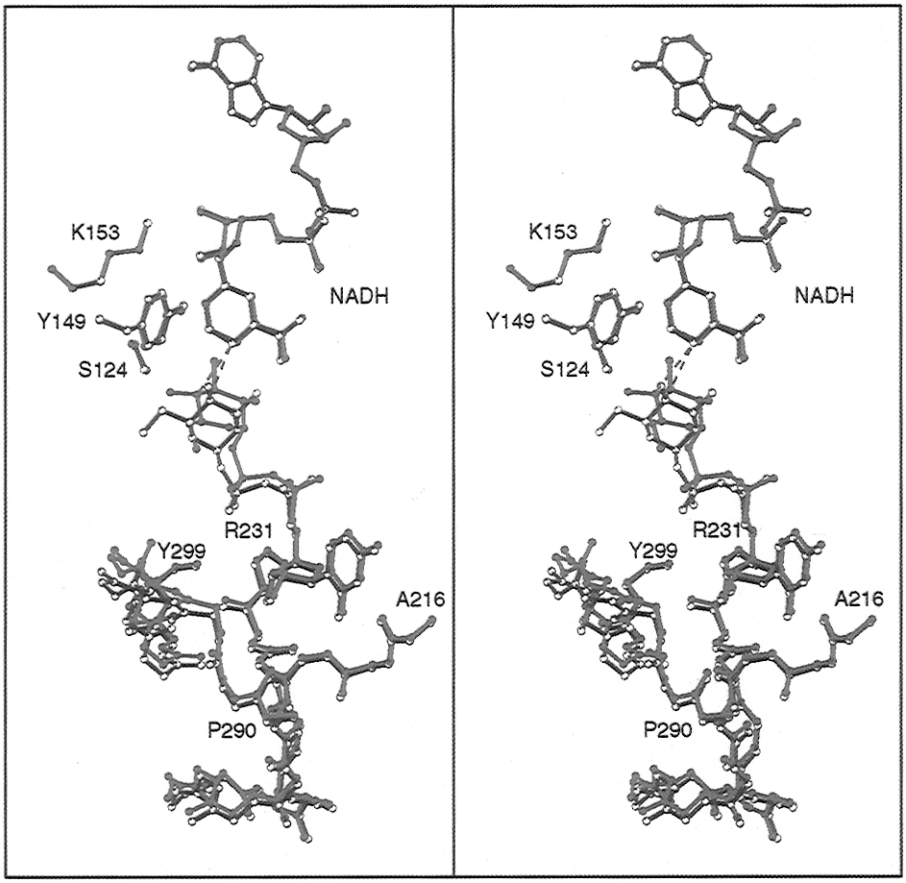

FIGURE 4: Superposition of the epimerase/NADH/UDP-mannose and epimerase/NADH/UDP-glucose models. The protein/UDP-mannose and protein/UDP-glucose complexes are displayed in black and red, respectively. The dashed lines indicate the direction of possible hydride transfer from C4 of the sugar moieties to C4 of the nicotinamide rings. The two models differ primarily in the position of the sugars and in the two regions of polypeptide chains defined by Ala 216 to Arg 231 and Pro 290 to Tyr 299. For the sake of clarity, only the polypeptide chain backbones are displayed for residues 216−231 and 290−299. Note that the conserved amino acids among the short-chain dehydrogenases, namely, Ser 124, Tyr 149, and Lys 153, adopt similar positions in both protein/UDP-sugar complexes.

the mannose is still positioned in the active site with the correct orientation for hydride transfer from C4 of the carbohydrate to C4 of the dinucleotide. In the epimerase/NADH/UDP-mannose and the epimerase/NADH/UDP-glucose complexes the distances between C4 of the sugar and C4 of the nicotinamide are 4.2 and 3.8 Å, respectively.

A cartoon of potential hydrogen bonds between the protein and the UDP-mannose is presented in Figure 5. The electrostatic interactions between epimerase and the uridine 5′-diphosphate are virtually identical to those observed in the epimerase/NADH/UDP-glucose complex. Due to the above-mentioned rotations, however, the mannose and glucose moieties interact with different protein side chain functional groups. Specifically, in the epimerase/NADH/UDP-glucose complex, $N^{\delta 2}$ of Asn 199, O^{η} of Tyr 149, O^{γ} of Ser 124, and O^{η} of Tyr 299 participate in hydrogen bonds to the 2′-, 3′-, 4′-, and 6′-hydroxyl groups of the glucose, respectively. In addition, the 6′-hydroxyl group of the glucose is anchored to the protein via $O^{\delta 1}$ of Asn 179 (Thoden *et al.*, 1996b). In the epimerase/NADH/UDP-mannose complex, both Asn 179 and Asn 199 likewise form hydrogen-bonding interactions with the mannose, albeit with different hydroxyl groups. As indicated in Figure 5, $O^{\delta 1}$ of Asn 179 lies within hydrogen-bonding distance of the 2′-hydroxyl group of the mannose while $N^{\delta 2}$ of Asn 199 interacts with the 3′-hydroxyl moiety. The close interaction between O^{γ} of Ser 124 and the 4′-hydroxyl group of glucose in the epimerase/NADH/UDP-glucose structure is not observed when UDP-mannose binds to the epimerase; rather the 4′-hydroxyl group interacts with an ordered water molecule. Also, the 6′-hydroxyl group of the mannose forms a hydrogen bond with O^{γ} of Thr 126 rather than with O^{η} of Tyr 299. In addition to these side chain functional groups, the carbonyl oxygen of Phe 178 forms a hydrogen bond with the 2′-hydroxyl group of the mannose.

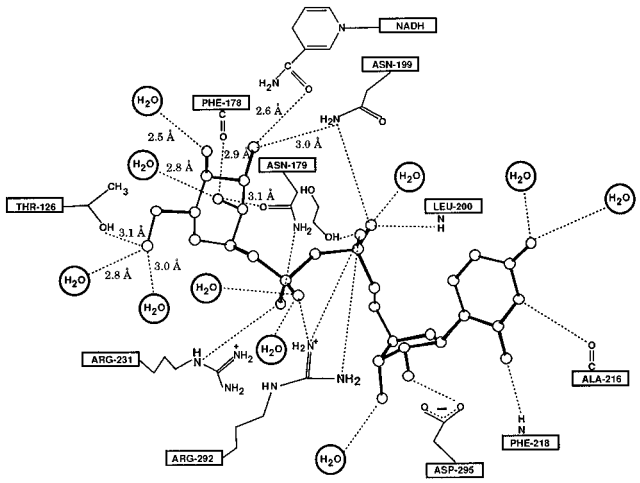

FIGURE 5: Schematic representation of potential hydrogen-bonding interactions between epimerase and UDP-mannose. Possible interactions between the protein and the ligand, within 3.2 Å, are indicated by the dashed lines. Distances between the sugar moiety and the protein are specifically indicated.

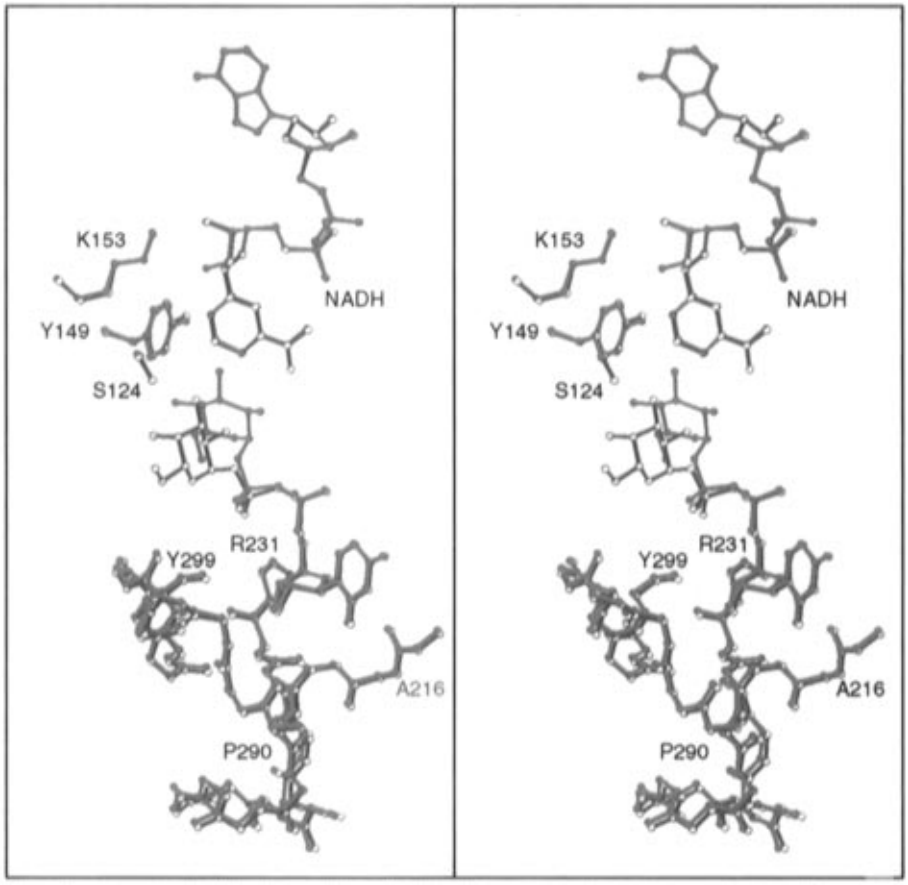

FIGURE 6: Superposition of the active site regions for the epimerase/NADH/UDP-fgal and epimerase/NADH/UDP-glucose complexes. The epimerase/NADH/UDP-fgal and epimerase/NADH/UDP-glucose models are displayed in black and red, respectively. The 4′-fluoro group is shown in yellow.

Description of the Epimerase/NADH/UDP-fgal Complex. Electron density corresponding the bound UDP-fgal substrate analog is displayed in Figure 3b. Average *B*-values for the protein and the solvent were 19.0 and 43.3 Å^2, respectively, while the average *B*-values for the UDP and the sugar portions of the substrate analog were 18.6 and 35.2 Å^2, respectively. The observed difference in temperature factors between the nucleotide and carbohydrate portion of the substrate analog suggests that either the sugar is more mobile in the active site or that partial hydrolysis of the UDP-fgal molecule occurs during the reduction/crystallization process. Experiments to address this issue are presently underway. As observed for the epimerase/NADH/UDP-mannose complex, the polypeptide chains for the enzyme/NADH/UDP-fgal and enzyme/NADH/UDP-glucose models are very similar with a root-mean-square deviation between their α-carbons of 0.15 Å.

A superposition of the epimerase/NADH/UDP-glucose and epimerase/NADH/UDP-fgal models is depicted in Figure 6. The UMP portions of the ligands coincide with a root-mean-square deviation of 0.18 Å. The major difference in conformation between the two UDP-sugar molecules occurs near the β-phosphorus atoms which are displaced, relative to one another, by 0.43 Å. In addition, there are changes in the dihedral angles defined by the α,β-bridging oxygen, the β-phosphorus, the glycosyl oxygen, and the hexose C1 and by the β-phosphorus, the glycosyl oxygen, the hexose C1, and C2 of approximately 107° and 20°, respectively. The C4 atoms of the sugars are separated by 2.8 Å. The observed hydrogen-bonding interactions between the epimerase and the UDP-fgal analog are indicated schematically in Figure 7. The most noticeable difference in the binding of the UDP-fgal molecule to epimerase is the lack of direct electrostatic interactions between protein side chains and the carbohydrate; rather the sugar is surrounded by ordered water molecules. These water molecules, however, function as bridges to various protein side chains and carbonyl oxygens. Specifically the water molecule that interacts with the 6′-hydroxyl group of the fluorinated galactose forms hydrogen bonds with O$^\gamma$ of Thr 126 and O$^\gamma$ of Ser 147 while the solvent positioned near the 2′-hydroxyl group of the sugar interacts with both

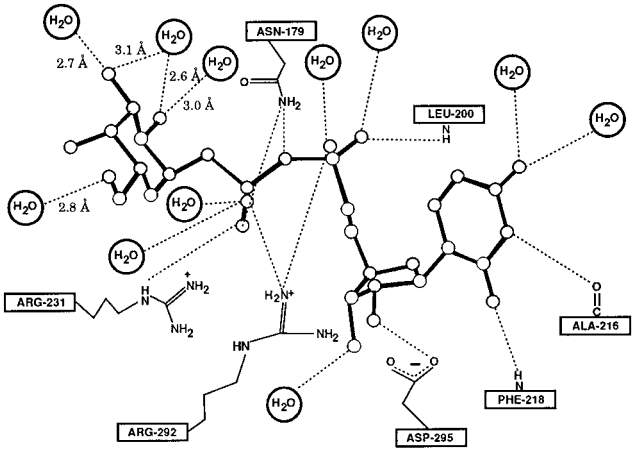

FIGURE 7: Schematic representation of potential hydrogen-bonding interactions between epimerase and UDP-fgal. Possible interactions between the enzyme and the substrate analog, within 3.2 Å, are indicated by the dashed lines.

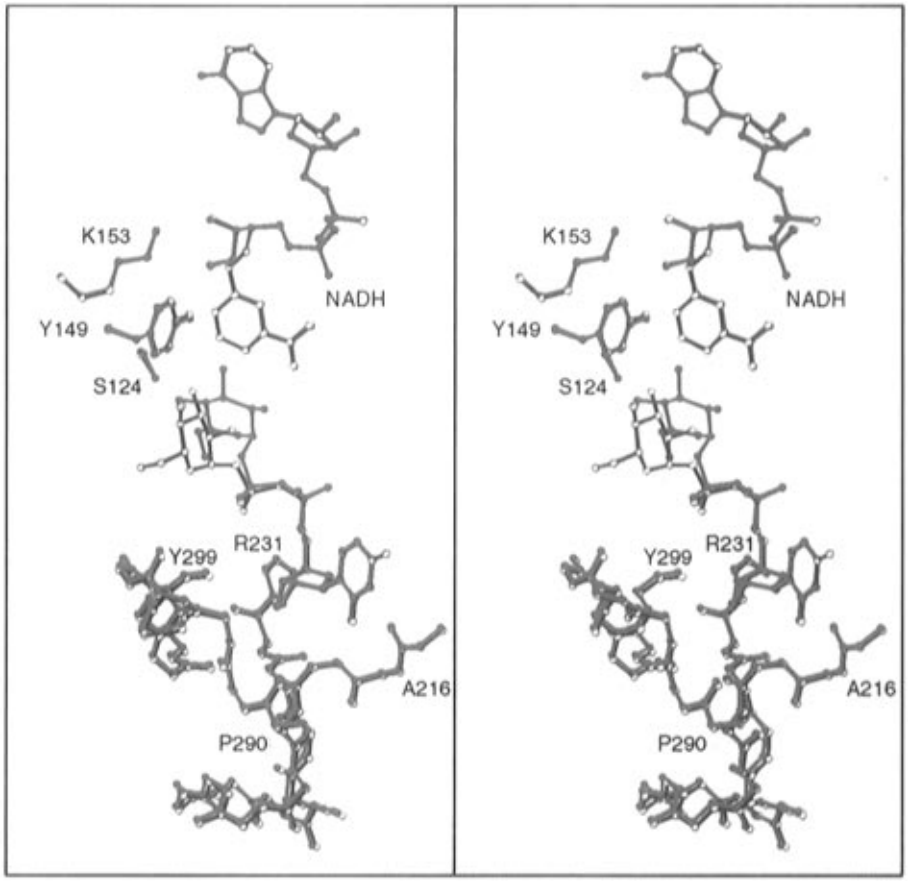

FIGURE 8: Superposition of the active site regions for the epimerase/NADH/UDP-fglu and epimerase/NADH/UDP-glucose models. The enzyme/NADH/UDP-fglu and enzyme/NADH/UDP-glucose complexes are displayed in black and red, respectively. The 4′-fluoro group is shown in yellow.

$O^{\delta 1}$ of Asn 179 and O^{η} of Tyr 299. There are two water molecules that surround the 3′-hydroxyl group of the sugar, and these, in turn, participate in electrostatic interactions with either O^{η} of Tyr 149 or O^{γ} of Ser 124 and the carbonyl oxygens of Tyr 177 and Phe 178. The 4′-fluoro group of the analog is located at 3.2 Å from O^{γ} of Thr 126.

Description of the Epimerase/NADH/UDP-fglu Complex. It was anticipated that the 4-deoxy-4-fluoro-α-D-galactose moiety would bind in the epimerase active site in essentially the same position as that observed for glucose, although rotated by approximately 180° about the bond connecting the β-phosphorus and the glycosyl oxygen. As described above, however, the fluorinated sugar is displaced from the glucose binding region. The question as to whether this resulted from fluorination at the C4 position or the fact that the analog was a derivative of galactose rather than glucose was addressed by cocrystallizing reduced epimerase in the presence of UDP-fglu.

Electron density corresponding to the bound substrate analog is shown in Figure 3c. Average *B*-values for the protein and the solvent were 25.4 and 47.9 $Å^2$, respectively. During the least-squares refinement of the model, several of the *B*-values for the carbohydrate moiety of the ligand assumed values exceeding 100 $Å^2$ whereas those for the nucleotide portion refined to an average temperature factor of 24.1 $Å^2$. Visual inspection of various electron density maps suggested that the occupancy of the sugar was approximately one-third that of the UDP portion. Refinement of the UDP-fglu molecule with the occupancy of the sugar set to one-third resulted in an average *B*-value of 27.6 $Å^2$ for the carbohydrate moiety. It appears that the fluorinated substrate analog is susceptible to hydrolysis, and experiments to test the structural integrity of the UDP-fglu molecule employed in this investigation are underway.

Regardless of whether the substrate analog was completely intact, the electron density clearly indicates that the binding site for the fluorinated glucose, as can be seen in Figure 8, is not the same as that observed for the natural substrate. The glucose and 4-deoxy-4-fluoro-α-D-glucose moieties are related to one another by rotations of approximately 115° and 13°, respectively, about the dihedral angles defined by the α,β-bridging oxygen, the β-phosphorus, the glycosyl oxygen, and the hexose C1 and by the β-phosphorus, the glycosyl oxygen, the hexose C1, and C2 of the carbohydrate. Due to such a rotation, the 4′-fluoro group, which was meant to mimic the 4′-hydroxyl group of glucose, is positioned at 5.0 Å from O^{γ} of Ser 124. Those electrostatic interactions involved in binding the substrate analog are depicted in Figure 9. As observed in the epimerase/NADH/UDP-fgal model, most of the interactions between the protein and carbohydrate portion of the UDP-fglu molecule are mediated through bridging water molecules. There are only two specific protein/sugar interactions observed, namely, those between the 2′- and 3′-hydroxyl groups of the hexose and O of Phe 178 and O^{γ} of Ser 124, respectively. Other than the differences shown in Figure 8, the polypeptide chains for the epimerase/NADH/UDP-glucose and epimerase/NADH/UDP-fglu complexes are nearly identical such that their α-carbons coincide with a root-mean-square deviation of 0.13 Å.

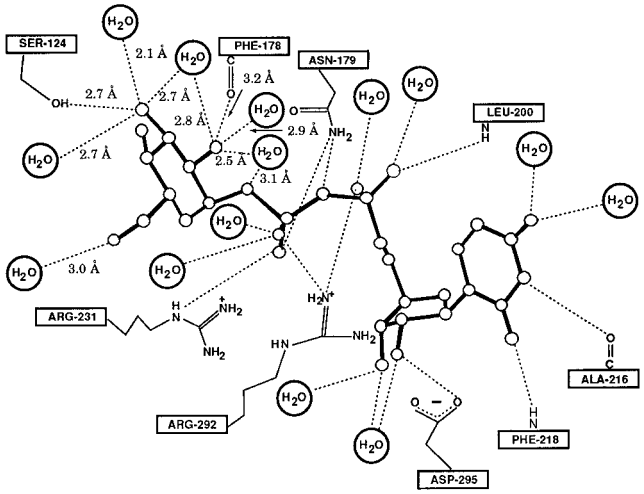

FIGURE 9: Schematic representation of potential hydrogen-bonding interactions between epimerase and UDP-fglu. Possible interactions between the enzyme and the substrate analog, within 3.2 Å, are indicated by the dashed lines.

DISCUSSION

A key issue regarding the catalytic mechanism of the epimerase is the manner by which nonstereospecific hydride transfer occurs between the *si* face of NAD^+ and C4 of the pyranosyl rings in UDP-galactose and UDP-glucose. Substrate binding experiments have revealed strong interactions between the epimerase and the nucleotidyl portions of the substrate but rather weak interactions between the enzyme and the pyranosyl moieties (Kang *et al.*, 1975; Wong & Frey, 1977). The most obvious interpretation from these studies is that the UDP moiety serves as an anchor to hold the weakly bound and presumably mobile pyranosyl group in the active site, thereby allowing either face of the 4-keto-pyranose ring to react with NADH as indicated in Scheme 1. Torsion about the bond linking the α-anomeric oxygen to the β-phosphorus of UDP can allow the required reorientation, and inspection of space-filling models indicates that nonstereospecificity of hydride transfer at pyranosyl C4 can be rationalized if the hydroxyl groups at C4 and C3 serve as the principal recognition points for the sugars in two orientations about this bond (Frey, 1987). The present X-ray structural studies of UDP-mannose, UDP-fgal, and UDP-fglu bound to epimerase/NADH more fully define the binding interactions at the pyranosyl site and support this model.

From binding and inhibition studies it is known that the interactions of uridine diphosphoryl compounds to epimerase are characterized by similar dissociation constants. For example, the dissociation constants for UDP-hexoses, UDP-pentoses, UDP-*p*-nitrophenol, UDP-*p*-(bromoacetamido)-phenol, and UDP-TEMPO range between 0.2 and 1.2 mM (Wong & Frey, 1977). The UDP substituents in this series range from polyhydroxylic to aromatic to both hydrophobic and bulky, yet all bind to the epimerase active site with comparable affinities. The 4-deoxy-4-fluoro substrate analogs UDP-fgal and UDP-fglu display K_i values of 1.4 and 1.2 mM, respectively, as competitive inhibitors (Chapeau & Frey, 1994), demonstrating that they, indeed, bind with affinities that are comparable both to each other and to other UDP compounds. The fact that epimerase binds all such UDP derivatives studied thus far with similar affinities indicates that the pyranosyl binding site contains few specific interactions between the sugar portion of UDP-ligand and the enzyme and that the site is clearly large enough to accommodate the motion required for the mechanism in Scheme 1.

The present X-ray structural results confirm the minimal enzyme/sugar interactions in the pyranosyl site and are consistent with the substrate structural mobility implied in Scheme 1. The different orientations in which the mannosyl, 4-deoxy-4-fluoroglucosyl, and 4-deoxy-4-fluorogalactosyl groups bind within the active site of epimerase show that there is adequate space to allow reorientation of the 4-keto-pyranosyl ring in the course of epimerization. Variations among the various sugar/protein complexes studied in this investigation are limited primarily in the dihedral angles about the α-anomeric oxygens and β-phosphorus and differences in the orientations of fixed water molecules around the sugar rings.

UDP-fglu and UDP-fgal may be regarded as analogs of UDP-4-ketoglucose, the intermediate in epimerization. Like the 4-keto group in the intermediate, the 4-fluoro substituent lacks the capacity to donate a hydrogen bond. In the small molecule structural analysis of methyl α-D-glucopyranoside, the 4′-hydroxyl group hydrogen of the sugar lies at 2.75 Å from a hydroxyl group oxygen of a neighboring molecule in the crystalline lattice (Berman & Kim, 1968). This interaction, however, is disrupted when the 4′-hydroxyl of the carbohydrate is replaced with fluorine, as demonstrated in the X-ray crystallographic analysis of methyl 4-deoxy-4-fluoro-α-D-glucopyranoside (Choong *et al.*, 1975). Whether the 4-fluoro group accepts hydrogen bonds as well as the 4-keto group is uncertain. In any case, both UDP-fglu and UDP-fgal are bound to the epimerase/NADH complex, as is the catalytic intermediate UDP-4-ketoglucose, and both bind differently from UDP-glucose, the principal difference being in the dihedral angles about the bond linking the α-anomeric oxygen with the β-phosphorus of UDP. In the epimerase/NADH/UDP-glucose abortive complex, the side chain of Ser 124 interacts directly with the sugar. The disruption of this one interaction, through the replacement of the 4′-hydroxyl group with fluorine, results in the fluorinated analog being oriented differently within the binding pocket. It seems likely that a 4-keto group would maintain its hydrogen-bonded contact with Ser 124. While the fluorinated analogs do not provide information about this, they do, however, demonstrate that an alteration in a single hydrogen-bonded contact at C4 leads to a large change in the dihedral angle about the α-anomeric oxygen and the β-phosphorus.

The axial 2′-hydroxyl group of mannose projecting from the β-face of the glycosyl ring in UDP-mannose forms a hydrogen bond with the carboxamide group of NADH that is absent with the other sugars studied in this investigation. This interaction forces a displacement of the mannosyl ring, its anomeric oxygen, and the β-phosphorus of UDP out of the active site to the extent that the contact of the 4′-hydroxyl group with the catalytic groups of Ser 124 and Tyr 149 is disrupted. This displacement is likely to be the reason for UDP-mannose not being a substrate, although C4 remains close enough to NAD^+ to allow reduction of the coenzyme (Nelsestuen & Kirkwood, 1971), presumably at a slow rate.

In galactose-1-phosphate uridylyltransferase from *E. coli*, another enzyme involved in galactose metabolism, the side chain positions for both Glu 317 and Gln 323 and the

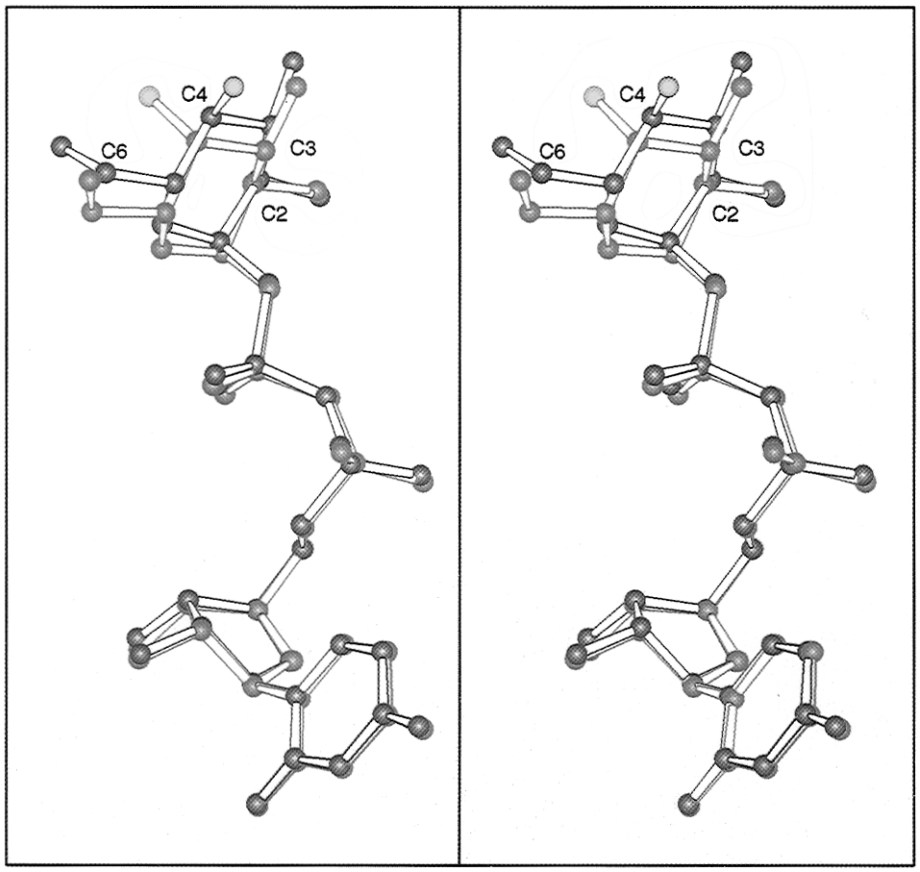

FIGURE 10: Superposition of the UDP-fglu and UDP-fgal molecules. The fluorinated glucose and galactose analogs are shown in blue and green, respectively. The 4′-fluoro group is displayed in yellow.

backbone dihedral angles of Val 314 are strictly dependent upon the identity of the sugar bound in the active site (Thoden *et al.*, 1996d). This is in sharp contrast to that observed for the epimerase, where the major structural differences among the epimerase/UDP-sugar complexes are strictly limited to the conformations of the ligands and in particular to two torsional angles. These dihedral angles can vary up to approximately 115° and 49°. Other than these differences, however, the epimerase/UDP-sugar complexes described here are so similar that all protein atoms for the UDP-mannose, UDP-fgal, and UDP-fglu models can be superimposed upon the epimerase/NADH/UDP-glucose abortive complex with root-mean-square deviations of 0.24, 0.21, and 0.18 Å, respectively. It appears that the epimerase is able to accommodate various carbohydrate moieties by local rearrangements of water molecules within the active site cleft, rather than by large changes in amino acid side chain conformations.

A comparison of the UDP-fgal and UDP-fglu molecules, as observed bound to the epimerase, is shown in Figure 10. While it has been postulated that UDP-glucose and UDP-galactose bind in the epimerase active site with the torsional angle about the β-phosphorus and the glycosyl oxygen differing by approximately 180° (Frey, 1987), these substrate analogs demonstrate that the corresponding 4-deoxy-4-fluoro sugars adopt very similar conformations with the dihedral angle differing by only 9°. The similar conformations may arise from the fact that the hydrogen-bonding capacity of the fluoro group is rather restricted. Whether the observed similarities in UDP-fglu and UDP-fgal binding to epimerase have implications for true substrate binding remains to be determined. Clearly, the structures of the epimerase complexed with UDP-galactose or some type of 4-ketopyranose intermediate analog would provide additional insight into the reaction mechanism of this fascinating enzyme, and experiments to prepare such crystalline complexes are in progress.

ACKNOWLEDGMENT

We thank Dr. W. W. Cleland for critically reading the manuscript and for helpful discussions throughout the course of this investigation.

REFERENCES

Azzi, A., Rehse, P. H., Zhu, D.-W., Campbell, R. L., Labrie, F., & Lin, S.-X. (1996) *Nat. Struct. Biol. 3*, 665−668.
Baker, M. E., & Blasco, R. (1992) *FEBS Lett. 301*, 89−93.
Bauer, A. J., Rayment, I., Frey, P. A., & Holden, H. M. (1992) *Proteins: Struct., Funct., Genet. 12*, 372−381.
Berman, H. M., & Kim, S. H. (1968) *Acta Crystallogr., Sect. B 24*, 897.
Caputto, R., Leloir, L. F., Trucco, R. E., Cardini, C. E., & Paladini, A. C. (1949) *J. Biol. Chem. 179*, 497−498.
Chapeau, M.-C., & Frey, P. A. (1994) *J. Org. Chem. 59*, 6994−6998.
Choong, W., Stephenson, N. C., & Stevens, J. D. (1975) *Cryst. Struct. Commun. 4*, 491.
Frey, P. A. (1987) in *Pyridine Nucleotide Coenzymes: Chemical, Biochemical, and Medical Aspects* (Dolphin, D., Poulson, R., & Avramovic, O., Eds.) pp 461−511, John Wiley & Sons, Inc., New York.
Ghosh, D., Weeks, C. M., Grochulski, P., Duax, W. L., Erman, M., Rimsay, R. L., & Orr, J. C. (1991) *Proc. Natl. Acad. Sci. U.S.A. 88*, 10064−10068.
Ghosh, D., Wawrzak, Z., Weeks, C. M., Duax, W. L., & Erman, M. (1994a) *Structure 2*, 629−640.
Ghosh, D., Erman, M., Wawrzak, Z., Duax, W. L., & Pangborn, W. (1994b) *Structure 2*, 973−980.

Ghosh, D., Pletnev, V. Z., Zhu, D.-W., Wawrzak, Z., Duax, W. L., Pangborn, W., Labrie, F., & Lin, S.-X. (1995) *Structure 3*, 503−513.
Glasfeld, A., Zbinden, P., Dobler, M., Benner, S. A., & Dunitz, J. D. (1988) *J. Am. Chem. Soc. 110*, 5152−5157.
Holm, L., Sander, C., & Murzin, A. (1994) *Nat. Struct. Biol. 1*, 146−147.
Jones, T. A., (1985) *Methods Enzymol, 115*, 157−171.
Kabsch, W. (1988a) *J. Appl. Crystallogr. 21*, 67−71.
Kabsch, W. (1988b) *J. Appl. Crystallogr. 21*, 916−924.
Kang, U. G., Nolan, L. D., & Frey, P. A. (1975) *J. Biol. Chem. 250*, 7099−7105.
Kraulis, P. J. (1991) *J. Appl. Crystallogr. 24*, 946−950.
Lemaire, H. G., & Müller-Hill, B. (1986) *Nucleic Acids Res. 14*, 7705−7711.
Lonchambon, F., Avenel, D., & Neuman, A. (1976) *Acta Crystallogr., Sect. B 32*, 1882.
Nelsestuen, G. L., & Kirkwood, S. (1971) *J. Biol. Chem. 246*, 7533−7543.
Reddy, B. S., Saenger, W., Mühlegger, K., & Weimann, G. (1981) *J. Am. Chem. Soc. 103*, 907−914.
Tanaka, N., Nonaka, T., Tanabe, T., Yoshimoto, T., Tsuru, D., & Mitsui, Y. (1996a) *Biochemistry 35*, 7715−7730.
Tanaka, N., Nonaka, T., Nakanishi, M., Deyashiki, Y., Hara, A., & Mitsui, Y. (1996b) *Structure 4*, 33−45.
Thoden, J. B., Frey, P. A., & Holden, H. M. (1996a) *Biochemistry 35*, 2557−2566.
Thoden, J. B., Frey, P. A., & Holden, H. M. (1996b) *Biochemistry 35*, 5137−5144.
Thoden, J. B., Frey, P. A., & Holden, H. M. (1996c) *Protein Sci. 5*, 2149−2161.
Thoden, J. B., Ruzicka, F. J., Frey, P. A., Rayment, I., & Holden, H. M. (1996d) *Biochemistry 35*, 1212−1222.
Tronrud, D. E., Ten Eyck, L. F., & Matthews, B. W. (1987) *Acta Crystallogr., Sect. A 43*, 489−501.
Varughese, K. I., Skinner, M. M., Whiteley, J. M., Matthews, D. A., & Xuong, N. H. (1992) *Proc. Natl. Acad. Sci. U.S.A. 89*, 6080−6084.
Varughese, K. I., Xuong, N. H., Kiefer, P. M., Matthews, D. A., & Whiteley, J. M. (1994) *Proc. Natl. Acad. Sci. U.S.A. 91*, 5582−5586.
Viswamitra, M. A., Post, M. L., & Kennard, O. (1979) *Acta Crystallogr., Sect. B 35*, 1089−1094.
Walsh, C. (1979) *Enzymatic Reaction Mechanisms*, Freeman, San Francisco.
Wilson, D. B., & Hogness, D. S. (1969) *J. Biol. Chem. 244*, 2132−2136.
Wong, S. S., & Frey, P. A. (1977) *Biochemistry 16*, 298−305.

BI970025J